Oncogene (2016) **35,** 2687–2697

www.nature.com/onc

ORIGINAL ARTICLE

Targeting MET and AXL overcomes resistance to sunitinib therapy in renal cell carcinoma

L Zhou[1], X-D Liu[1], M Sun[1], X Zhang[1], P German[1], S Bai[1], Z Ding[1], N Tannir[1], CG Wood[2], SF Matin[2], JA Karam[2], P Tamboli[3], K Sircar[3], P Rao[3], EB Rankin[4], DA Laird[5], AG Hoang[3], CL Walker[6], AJ Giaccia[4] and E Jonasch[1]

Antiangiogenic therapy resistance occurs frequently in patients with metastatic renal cell carcinoma (RCC). The purpose of this study was to understand the mechanism of resistance to sunitinib, an antiangiogenic small molecule, and to exploit this mechanism therapeutically. We hypothesized that sunitinib-induced upregulation of the prometastatic MET and AXL receptors is associated with resistance to sunitinib and with more aggressive tumor behavior. In the present study, tissue microarrays containing sunitinib-treated and untreated RCC tissues were stained with MET and AXL antibodies. The low malignant RCC cell line 786-O was chronically treated with sunitinib and assayed for AXL, MET, epithelial–mesenchymal transition (EMT) protein expression and activation. Co-culture experiments were used to examine the effect of sunitinib pretreatment on endothelial cell growth. The effects of AXL and MET were evaluated in various cell-based models by short hairpin RNA or inhibition by cabozantinib, the multi-tyrosine kinases inhibitor that targets vascular endothelial growth factor receptor, MET and AXL. Xenograft mouse models tested the ability of cabozantinib to rescue sunitinib resistance. We demonstrated that increased AXL and MET expression was associated with inferior clinical outcome in patients. Chronic sunitinib treatment of RCC cell lines activated both AXL and MET, induced EMT-associated gene expression changes, including upregulation of Snail and β-catenin, and increased cell migration and invasion. Pretreatment with sunitinib enhanced angiogenesis in 786-0/human umbilical vein endothelial cell co-culture models. The suppression of AXL or MET expression and the inhibition of AXL and MET activation using cabozantinib both impaired chronic sunitinib treatment-induced prometastatic behavior in cell culture and rescued acquired resistance to sunitinib in xenograft models. In summary, chronic sunitinib treatment induces the activation of AXL and MET signaling and promotes prometastatic behavior and angiogenesis. The inhibition of AXL and MET activity may overcome resistance induced by prolonged sunitinib therapy in metastatic RCC.

Oncogene (2016) **35,** 2687–2697; doi:10.1038/onc.2015.343; published online 14 September 2015

INTRODUCTION

Renal cell carcinoma (RCC) is an epithelial tumor derived from the proximal tubules of nephrons.[1] The major subtype of RCC (~75%) is clear cell RCC (ccRCC).[2] Clinically, antiangiogenic therapy is a major treatment modality for metastatic RCC, targeting the vascular endothelial growth factor (VEGF) ligand itself with anti-VEGF antibodies such as bevacizumab or inhibiting proangiogenic receptor tyrosine kinases (RTKs) with small-molecule inhibitors such as sunitinib, pazopanib or axitinib.[3] Unfortunately, between 10% and 20% of patients have tumors that are refractory to antiangiogenic therapy, and a large majority of the remaining patients eventually demonstrate tumor growth after a median of 10–12 months of therapy.[4] Discontinuation of sunitinib treatment in RCC patients results in the rapid reappearance of angiogenesis. Very few patients achieve complete response, and death from metastatic RCC occurs at a median of 2 years after diagnosis.[4]

The determinants of response and resistance to antiangiogenic therapy in RCC are poorly understood. Regardless of which antiangiogenic therapy is being used, the changes that are occurring in the tumor microenvironment must ultimately impact the endothelial phenotype, the main target of antiangiogenic therapy. Studies of relative sensitivities of RCC tumor and endothelium to antiangiogenic therapy in model systems have shown that the tumor cell is only minimally affected by sunitinib, whereas endothelial cells are quite sensitive.[5] However, chronic treatment with antiangiogenic therapy may have sublethal effects on tumor cells themselves, which induce counter-regulatory alterations in cell signaling that ultimately affect the efficacy of antiangiogenic therapy. Factors that alter the tumor microenvironment and engender resistance may include cancer cell-specific changes, which include activation of the PI3K (phosphoinositide-3 kinase) signaling pathway within the tumor,[6–8] induction of prometastatic pathways or enhanced production of proangiogenic factors by the tumor. The search for tumor cell-specific effector molecules that can impart therapeutic resistance to antiangiogenic agents has provided several candidates, including the MET and AXL RTKs.[9]

MET is a RTK that can be dysregulated by gene mutation, gene amplification and protein overexpression and through a ligand-dependent autocrine or paracrine loop.[10–12] Increased total MET as well as phospho-MET are associated with worse outcome in

[1]Department of Genitourinary Medical Oncology, The University of Texas MD Anderson Cancer Center, Houston, TX, USA; [2]Department of Urology, Division of Surgery, The University of Texas MD Anderson Cancer Center, Houston, TX, USA; [3]Department of Pathology, The University of Texas MD Anderson Cancer Center, Houston, TX, USA; [4]Department of Radiation Oncology, Stanford University School of Medicine, Stanford, CA, USA; [5]Exelixis Inc., South San Francisco, CA, USA and [6]Institute of Biosciences and Technology, Texas A&M Health Science Center, Houston, TX, USA. Correspondence: Professor E Jonasch, Department of Genitourinary Medical Oncology, The University of Texas MD Anderson Cancer Center, 1155 Hermann Pressler Drive, Houston, TX 77030, USA.
E-mail: ejonasch@mdanderson.org
Received 23 March 2015; revised 5 August 2015; accepted 7 August 2015; published online 14 September 2015

both ccRCC and nonclear cell RCC.[13–15] However, there has not been a rigorous investigation of the inducibility of MET activation in the face of antiangiogenic therapy in RCC to determine whether either innate or induced MET expression is a mechanism of resistance to antiangiogenic treatment. Previous studies have shown that treatment of pancreatic neuroendocrine tumors in RIPTag2 mice with a neutralizing antiangiogenic antibody reduced tumor burden but increased MET activation, increased invasion and induced metastases. Interestingly, invasion and metastases were reduced by concurrent inhibition of MET by PF-04217903 or PF-02341066 (crizotinib). A similar benefit was found in orthotopic Panc-1 pancreatic carcinomas treated with sunitinib plus PF-04217903 and in RIP-Tag2 tumors treated with cabozantinib.[16]

In addition to MET, AXL has emerged as a biomarker and therapeutic target for a variety of metastatic cancers.[17–19] AXL belongs to the TAM family of RTKs where GAS6 is the common ligand. GAS6/AXL stimulates multiple protumorigenic signaling cascades, including those that promote cellular adhesion, invasion, migration, pro-inflammatory cytokine production, antiapoptosis, proliferation and survival.[20–24] AXL expression was found to be increased in RCC compared with matched normal kidney tissue at the mRNA level.[25] In RCC patients, AXL levels are associated with tumor progression and reduced patient survival.[26] Most recently, a role for AXL in the regulation of MET and epidermal growth factor receptor signaling was described, indicating that AXL may also function as an important factor mediating resistance against TKIs.[20–24] Furthermore, AXL signaling is essential for VEGF-mediated activation of PI3K/AKT and migration of endothelial cells, indicating that AXL may also be a mechanism of resistance to antiangiogenic therapies.[24] Despite the critical role of AXL in cancer development and metastasis, its role in the development of resistance to antiangiogenic therapy is unknown.

In the present study, we investigated the effects of chronic treatment of RCC cells with sunitinib on both AXL and MET signaling, as well as epithelial–mesenchymal transition (EMT) and angiogenic and prometastatic behavior. The blockage of AXL and MET activation by either cabozantinib treatment or specific short hairpin RNA (shRNA) knockdown suppressed the EMT phenotype and VEGF secretion induced by chronic sunitinib treatment. We also show that chronic pretreatment of cell lines with sunitinib conferred a more aggressive tumor phenotype when implanted in mice, which was tightly associated with upregulation of MET and AXL. Rescue of sunitinib resistance in tumors was possible with administration of cabozantinib, a dual VEGF and MET inhibitor. Our results suggest that chronic sunitinib treatment induces antiangiogenic therapy resistance through the activation of AXL and MET signaling and that the suppression of AXL and MET activation in the epithelial cancer cell could be an important strategy to prevent antiangiogenic therapy resistance.

RESULTS

AXL protein levels were elevated in sunitinib-treated ccRCC patient tumors

By analyzing AXL expression in ccRCC tumor samples that were treated with sunitinib and comparing them to non-treated controls, we found sunitinib-treated tumors exhibited increased AXL protein levels (Figure 1a). Increased AXL levels were previously reported to be associated with poor survival in RCC patients.[26] We examined the correlation between AXL and patient progression-free survival and overall survival (OS) in sunitinib-treated patients. As demonstrated in Figure 1b, higher AXL expression in RCC tumor cells is associated with shorter OS. Higher AXL levels are associated with a trend toward shorter progression-free survival, with a *P*-value of 0.072.

Higher MET levels correlated with poor OS and progression-free survival

Higher MET expression was previously reported to occur in RCC compared with adjacent normal kidney tissue, and higher MET expression correlated with worse disease-specific survival.[13] In our RCC tumor samples, higher MET expression correlated with decreased OS and progression-free survival in both control and sunitinib-treated cohorts (Figure 1d). Treatment with sunitinib did not alter total MET expression in our sample set (Figure 1c).

Elevated AXL and MET signaling was observed in RCC cells chronically treated with sunitinib

Although antiangiogenic agents were designed to target the tumor endothelium and stroma, these agents may also have an impact on the epithelial cancer cells themselves. In an effort to elucidate tumor cell autonomous mechanisms of antiangiogenic therapy resistance, we specifically sought to determine whether sunitinib treatment altered AXL and MET signaling in 786-O and other ccRCC cell lines. To understand the effect of long-term VEGF receptor inhibition on tumor cell biology, we treated RCC cell lines with both short-term (24 hour) and chronic (>2 weeks) sunitinib therapy. We observed that sunitinib treatment elevated AXL expression in 786-O cells (Figure 2a, second panel) as well as in A498 and RCC4 lines (Supplementary Figure S1). In addition to increased total AXL protein levels, elevated AXL activity (as indicated by increased phospho-AXL-Y702 levels[27,28]) was observed after sunitinib treatment (Figure 2a, first panel). Phospho-MET-1234/5 levels were suppressed by short-term sunitinib treatment (1 day) but recovered with chronic sunitinib treatment (Figure 2a, third panel). To evaluate the optimal treatment duration and dose, we performed dose curve and time course assay and found that 1μM sunitinib can induce sunitinib resistance in 2 weeks (Supplementary Figure S2). In addition to the rebound of AXL and MET receptors, their downstream target kinases, including AKT and extracellular signal–regulated kinase (ERK), were activated with chronic sunitinib treatment (Figure 2a, sixth and seventh panels). Clinically, after a period of sunitinib treatment, patients usually take treatment breaks. Thus we also tested the effect of sunitinib deprivation on sunitinib chronically treated 786-O cells. Surprisingly, AXL levels were maintained, the activity of MET remained elevated and the activation of AXL/MET downstream kinases AKT and ERK persisted (Figure 2a, column 4).

GAS6, the AXL ligand, is found high in the serum of RCC patients and is correlated with poor prognosis.[26,29] High hepatocyte growth factor (HGF) levels and intracellular MET pathway activation were also correlated with poor prognosis in patients with RCC.[30] We directly assessed the effect of MET and AXL ligands on downstream signaling pathways. As seen in Figure 2b, the activity of AKT and ERK in chronic sunitinib-treated cells were highly stimulated by the MET ligand HGF and the AXL ligand GAS6. This result suggests that, although chronic sunitinib treatment did not augment MET receptor levels, MET downstream signaling was sensitized, possibly by signaling molecules such as the Src family kinases,[9,31–33] which were activated by chronic sunitinib treatment (Figure 2a, panel 5). The western blotting from GAS6/HGF-stimulated AXL/MET signaling cascades also suggested that chronic sunitinib treatment augmented Src activation as indicated by increased Src phosphorylation (Figure 2b, fifth panel).

EMT signaling was induced with chronic sunitinib treatment

EMT has an important role in tumor metastasis. EMT signaling is regulated by AKT through the suppression of glycogen synthase kinase 3β (GSK3β).[34] We investigated whether sunitinib affected ccRCC EMT by checking the expression or phosphorylation levels of the EMT signaling proteins, including GSK3β, β-catenin and SNAIL.[34–36] We discovered that phospho-GSK3b-serine9 is stimulated

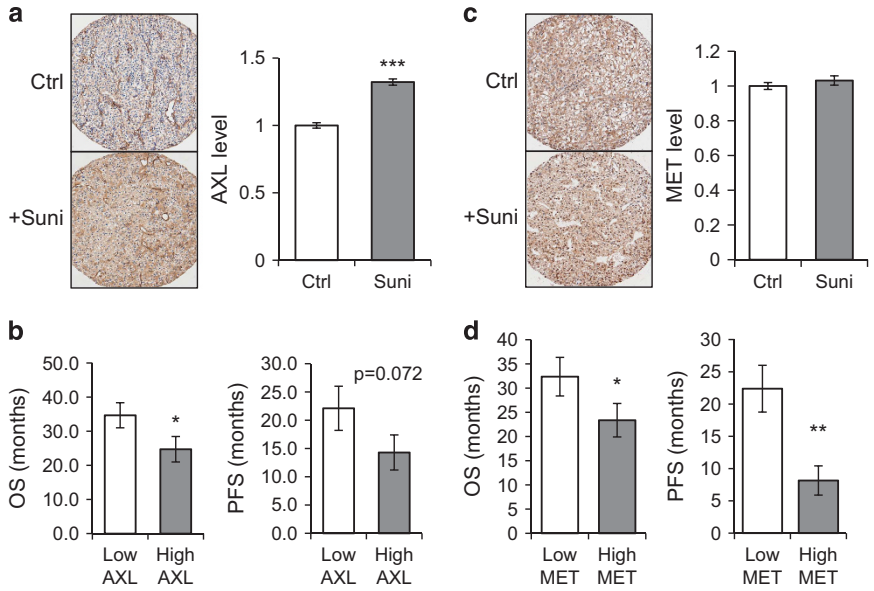

Figure 1. Sunitinib therapy increased AXL level in RCC tumors. AXL and MET expression are associated with worse OS in RCC patients. (**a**) Tissue microarray (TMA) from sunitinib-treated or untreated tumor from RCC patients were stained for AXL. The AXL levels were quantified and compared between the two groups of patients (***$P < 0.001$). (**b**) The sunitinib-treated patients were equally separated to high and low groups according to the AXL levels; the OS and progression-free survival (PFS) were compared between the two groups (*$P < 0.05$). (**c**) TMA from sunitinib-treated or untreated tumor from RCC patients were stained for MET. The AXL levels were quantified and compared between the two groups of patients. (**d**) The sunitinib-treated patients were equally separated to high and low groups according to the MET levels; the OS and PFS were compared between the two groups (*$P < 0.05$, **$P < 0.01$).

by chronic sunitinib treatment and persists after removal of sunitinib after chronic treatment (Figure 2a, eighth panel). The expression of SNAIL (Figure 2a, ninth panel) and β-catenin (Figure 2a, tenth panel) are induced in a similar pattern. These findings suggest chronic sunitinib treatment promotes prolonged cellular EMT signaling.

Chronic sunitinib treatment promoted cell migration and invasion

Cell migration has an important role in cancer metastasis, to which both MET and AXL contribute.[21,35,37] In wound-healing experiments, we found that chronic sunitinib-treated cells migrated faster than parental cells, which could not be effectively suppressed by re-introducing sunitinib. (Figure 2c). In contrast, sunitinib-treated parental cells exhibited reduced migration (Figure 2c, upper right panel), which is also observed in breast cancer cell lines.[38] This could be the result of sunitinib-activated EMT signaling, which is dependent on either the activation of MET[35,37] or AXL[21] that have been observed in other cancer cells. We further examined the effect of chronic sunitinib treatment on 786-O ccRCC cell invasion as outlined in Figure 2d. Chronically sunitinib-treated cells demonstrated significantly higher invasion ability in Matrigel-coated transwells (Figure 2d), and re-treatment with sunitinib could not effectively suppress cell invasion. The development of drug resistance has a major role in the proliferative ability of cancer cells. As demonstrated in Supplementary Fig S3A, the chronic sunitinib-treated 786-O cells were more resistant to retreatment with sunitinib. We also found chronic sunitinib-treated 786-O cells were more resistant to cytotoxicity and apoptosis induced by high dose (2–20 μM) sunitinib treatment (Supplementary Figures S3B–D).

Chronic sunitinib treatment-induced RCC EMT phenotypes are AXL and MET dependent

We next asked whether the induction of EMT-promoting genes was AXL and MET dependent by genetically blocking AXL and MET expression with specific shRNA. Our data indicate that EMT signaling was impaired by suppression of AXL or MET expression (Figure 3a). Moreover, AXL and MET pathways are induced in sunitinib-treated cells upon Gas6 and HGF addition (Figure 3b). The suppression of AXL and MET expression also decreased chronic sunitinib treatment-induced cell migration and invasion (Figures 3c and d), although cell proliferation and apoptosis were unaffected (Supplementary Figure S4). These results suggest that through the activation of AXL and MET chronic sunitinib treatment promotes EMT signaling to promote cell migration and invasion but not cell proliferation.

Cabozantinib inhibited AXL and MET activation

Recently, a novel RTK inhibitor, cabozantinib, which can potently inhibit MET and AXL receptors' activity, has shown clinical activity in a small cohort of heavily pretreated RCC patients.[39] A phase III study is currently underway comparing cabozantinib with everolimus in patients with advanced RCC who progressed after prior VEGF RTK therapy (NCT01865747). We tested whether cabozantinib could suppress chronic sunitinib treatment-induced AXL or MET signaling activation or re-activation. Cabozantinib treatment abolished both AXL and MET activation (Figure 4a) in sunitinib chronically treated 786-O cells. The activation of the downstream signaling molecules, including AKT and ERK, was also suppressed. The expression of EMT marker proteins, Snail and β-catenin, were reduced (Figure 4a). Ligand-induced AXL and MET signaling stimulation were blocked by cabozantinib treatment (Figure 3b). We further investigated the effect of cabozantinib on cell migration and invasion on chronic sunitinib-pretreated 786-O cells and parental 786-O cells. We found that cabozantinib effectively reduced cell migration and invasion, which were augmented by chronic sunitinib treatment (Figures 4c and d). Of note, cabozantinib treatment did not change the cell proliferation rate in either the parental cells or the chronic sunitinib-pretreated cells (Supplementary Figure S5).

Besides MET and AXL, cabozantinib also suppresses other RTKs, including KIT, RET and TIE2.[40,41] To characterize whether these RTKs are involved in the development of sunitinib resistance and potentially be targeted by cabozantinib, we examined the effect of chronic sunitinib treatment on the activation of these RTKs

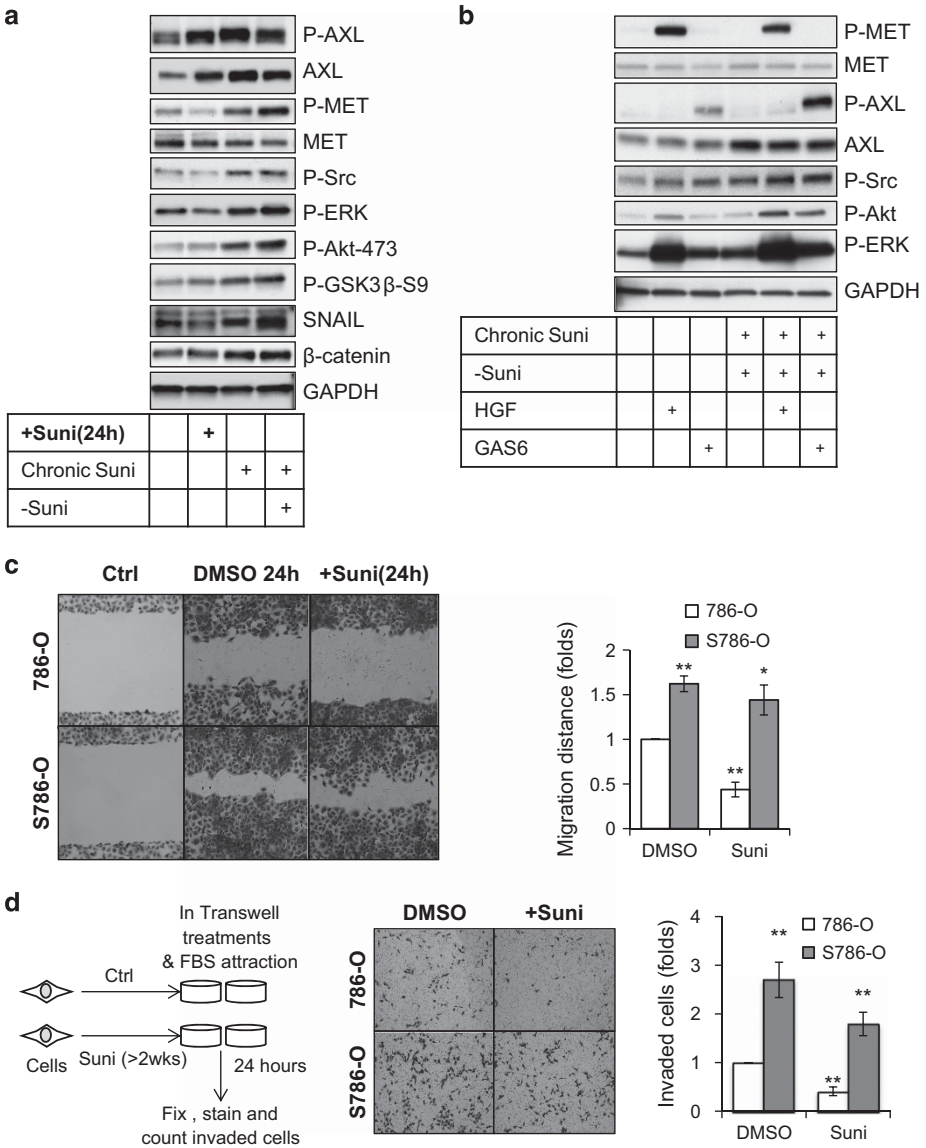

Figure 2. Chronic sunitinib treatment potentiates RCC cell EMT. (**a**) 786-O cells were acutely treated with sunitinib (+Suni, 1 μM, 24 h) or chronically treated with sunitinib (Chronic Suni, 1 μM, >2weeks) as indicated. The cells in the last lane were treated in sunitinib-free media for 4 days (−Suni) before lysis. Cell lysates were examined by western blotting with specific antibodies as indicated. Data represent three independent experiments. (**b**) Chronic sunitinib-pretreated cells were treated in sunitinib-free media for 3 days. The cells and 786-O parental cells were then serum starved for 24 h followed by HGF (100 ng/ml, 30 min) or GAS6 (200 ng/ml, 30 min) stimulation. The cells were then lysed and examined by western blotting with specific antibodies as indicated. To better visualize the phosphorylated MET and AXl signal with HGF and GAS6 stimulation, shorter exposure time was used compared with the blots in panel (**a**). Data represent three independent experiments. (**c**) 786-O cells that were chronically pretreated with sunitinib were deprived of sunitinib (S786-O) and the cells and 786-O parental cells were then seeded for wound-healing experiment as described in Materials and methods. The cells were treated with DMSO or sunitinib (1 μM, 24 h) as indicated. The migration distances from four independent experiments were measured and analyzed by comparing to the migration distance of 786-O cells with DMSO treatment (*$P < 0.05$, **$P < 0.01$). (**d**) The transwells were coated with Matrigel as described in Materials and methods. Chronic sunitinib-pretreated 786-O that were deprived of sunitinib (S786-O) or 786-O parental cells (10 000 per well) were seeded in the transwells in serum-free medium supplied with sunitinib (Suni, 1 μM) or DMSO as indicated, and the complete growth medium with sunitinib (1 μM) or DMSO was added to the bottom wells. After 24 h, the invading cells were stained and counted as described in Materials and methods. The invading cell numbers from four independent experiments were compared with untreated cells. (**$P < 0.01$).

with or without the suppression of AXL or MET by shRNA. The results suggested that, with the conditions we generated, the activities of these RTKs are unaffected (Supplementary Figure S6).

Chronic sunitinib treatment promoted AXL- and MET-dependent angiogenesis

The suppression of angiogenesis by anti-VEGF medicine is a mainstay of metastatic RCC treatment. We next examined whether chronic sunitinib treatment affected angiogenesis through modulating RCC cell function. We studied the communication between RCC and endothelial cells by co-culturing 786-O cells with human umbilical vein endothelial cells (HUVECs). As a functional end point, we examined HUVEC tube formation. HUVEC cells co-cultured with chronic sunitinib-pretreated 786-O cells formed more tubes, and the ablation of AXL or MET by shRNA reduced HUVEC tube formation (Figure 5a). These results indicate that chronic sunitinib pretreatment of RCC cells may promote angiogenesis through AXL- and

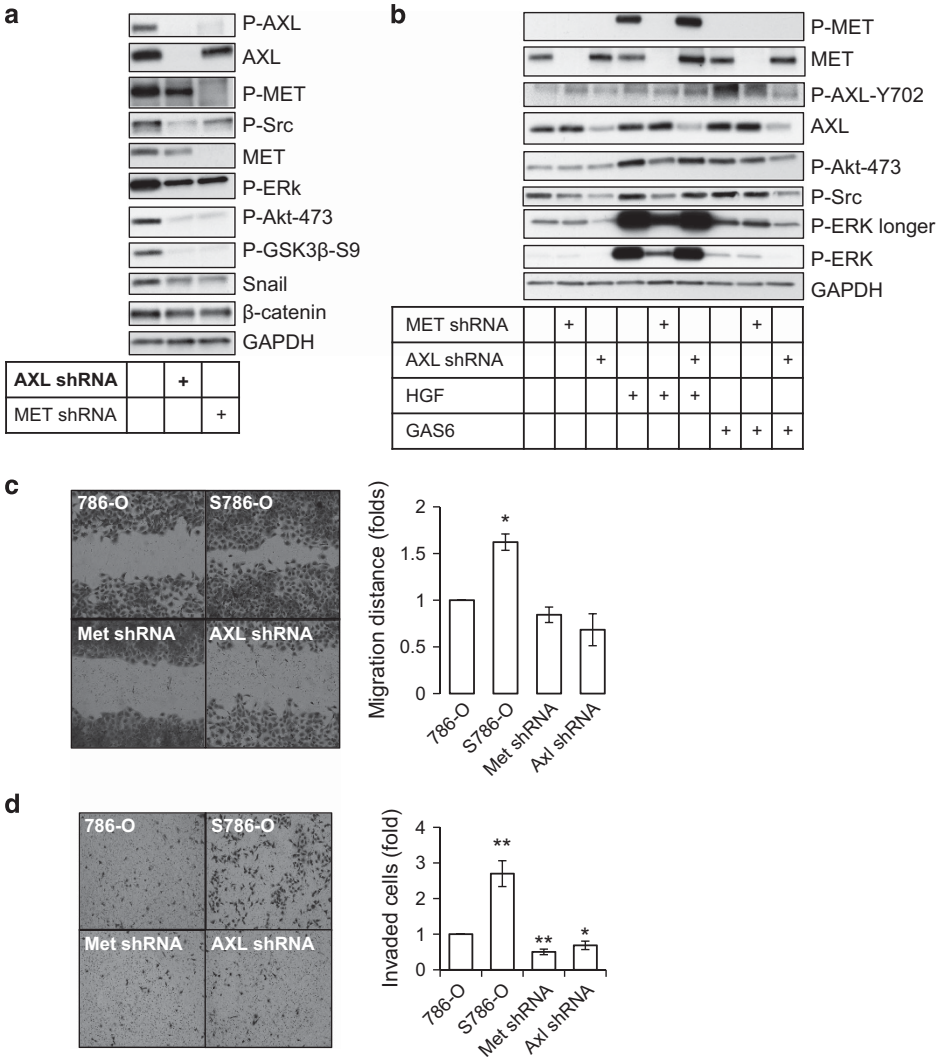

Figure 3. Chronic sunitinib treatment-induced EMT is AXL and MET dependent. (**a**) 786-O cells, 786-O cells that stably expressed *AXL* or *MET* shRNA constructs were chronically treated with sunitinib (1 μM) and then deprived of sunitinib for 48 h. The cells were examined by western blotting with specific antibodies as indicated. Data represent three independent experiments. (**b**) Chronic sunitinib-pretreated cells (786-O, *AXL* shRNA and *MET* shRNA) were deprived of sunitinib for 3 days. The cells and 786-O parental cells were then serum starved for 24 h followed by HGF (100 ng/ml, 30 min) or GAS6 (200 ng/ml, 30 min) stimulation as indicated. The cells were then lysed and examined by western blotting with specific antibodies as indicated. Data represent three independent experiments. (**c**) 786-O cells, 786-O cells that were stably infected with *AXL* or *MET* shRNA constructs were chronically treated with sunitinib (1 μM) and then deprived of sunitinib, and 786-O parental cells were seeded for wound-healing experiment as described in Materials and methods. The gap distances in four independent experiments were measured and analyzed (*$P < 0.05$). (**d**) The transwells were coated with Matrigel as described in Materials and methods. 786-O cells, 786-O cells that were stably infected with *AXL* or *MET* shRNA constructs were chronically treated with sunitinib (1 μM) and then deprived of sunitinib, and 786-O parental cells were seeded (10 000 per well) in the transwells in serum-free medium. Complete Growth Medium was added to the bottom wells. After 24 h, the invading cells were stained and counted as described in Materials and methods. The data in this figure are representative for three shRNA constructs designed to target different sequences in *MET* and *AXL* (*$P < 0.05$, **$P < 0.01$).

MET-dependent mechanisms. We then examined the ability of sunitinib and cabozantinib to suppress HUVEC tube formation in the co-culture system and discovered that the re-introduction of sunitinib reduced HUVEC tube formation in the sunitinib-pretreated system to a similar level as in untreated parental system (Figure 5b), but cabozantinib treatment reduced tube formation in both of the co-culture systems (Figure 5b) and decreased HUVEC tube formation more than sunitinib treatment.

HUVEC tube formation depends on environmental VEGF levels. We determined whether sunitinib pretreatment altered VEGF secretion from RCC cells. Our results suggest that chronic sunitinib treatment elevated VEGF level in conditioned medium, whereas the knockdown of AXL and MET impaired VEGF secretion (Figure 5c). The inhibition of AXL and MET signaling by cabozantinib also suppressed VEGF secretion to conditioned medium (Figure 5d).

Chronic sunitinib pretreatment potentiates tumor growth and angiogenesis in a xenograft mouse model

To investigate the *in vivo* effect of chronic sunitinib treatment, we established two chronic sunitinib-treated xenograft mouse models. For the first model, we injected chronic sunitinib-pretreated 786-O cells and parental 786-O cells into the opposite flanks of nude mice. We found that the sunitinib-pretreated cells produced faster-growing tumors (Figure 6a). In addition, the AXL and MET signaling cascades were elevated in the pretreated tumors as shown by increased phospho-AXL-702, phospho-MET-1234/5, phospho-AKT-473, phospho-ERK-202/4 and phospho-GSK3β-9

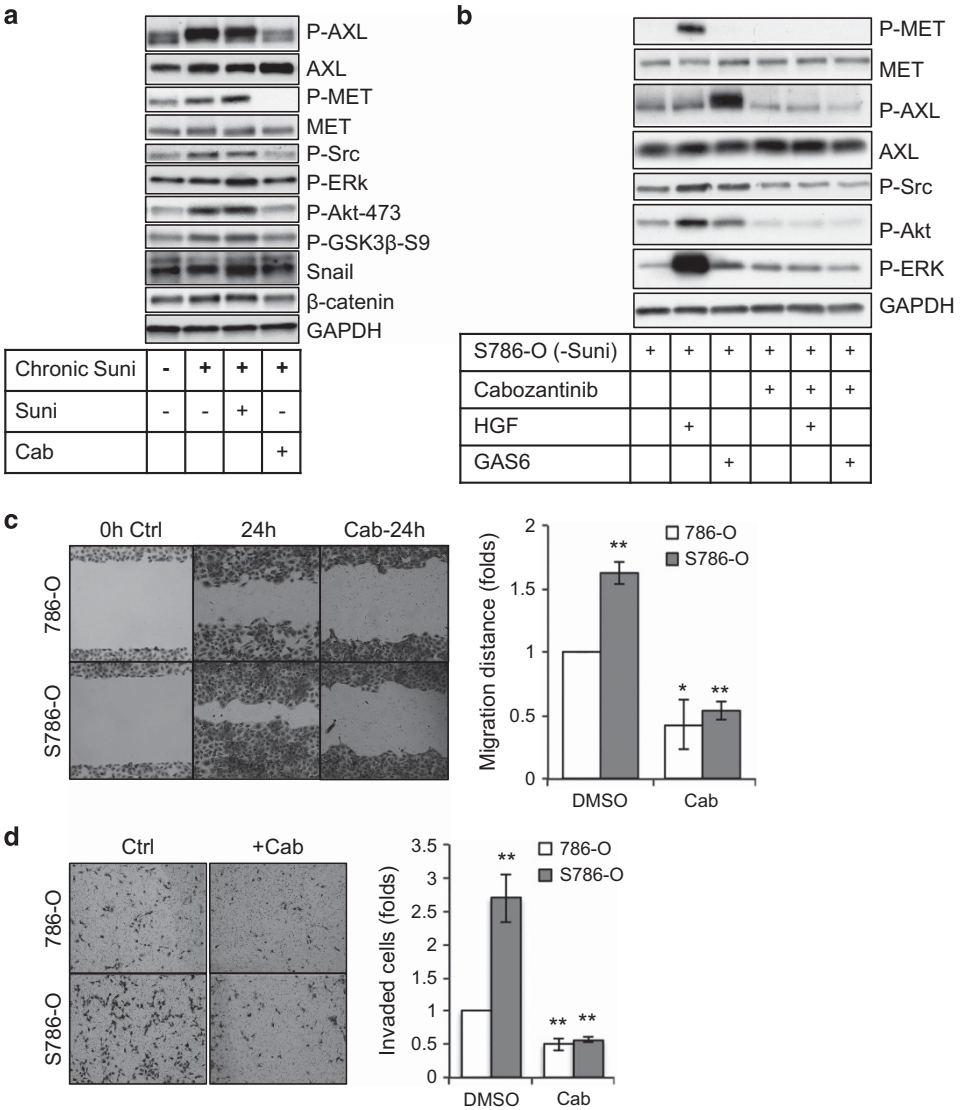

Figure 4. Cabozantinib suppressed MET/AXL signaling and chronic sunitinib treatment-induced EMT. (**a**) Chronic sunitinib-treated 786-O cells and 786-O parental cells were cultured in medium with or without sunitinib (1 μM) for 3 days and then treated with or without cabozantinib (5 μM, 24 h) as indicated. The cells were lysed and examined by western blotting with specific antibodies as indicated. Data represent three independent experiments. (**b**) Chronic sunitinib-treated 786-O cells were cultured in medium without sunitinib for 3 days and then treated with cabozantinib (5 μM, 24 h) as indicated in serum-free medium. The cells were then stimulated by HGF (100 ng/ml, 30 min) or GAS6 (200ng/ml, 30 min). The cells were then lysed and examined by western blotting with specific antibodies as indicated. Data represent three independent experiments. (**c**) Chronic sunitinib-treated 786-O cells and 786-O parental cells were cultured in medium without sunitinib before experiment. The cells were then seeded for wound-healing experiment as described in Materials and methods. The cells were treated with DMSO or cabozantinib (5 μM, 24h) as indicated. The gap distances in four independent experiments were measured and analyzed (*$P < 0.05$, **$P < 0.01$). (**d**) The transwells were coated with Matrigel as described in Materials and methods. Chronic sunitinib-pretreated 786-O cells that were deprived of sunitinib (S786-O) or 786-O parental cells (10 000 per well) were seeded in transwells in serum-free medium supplied with cabozantinib (Cab, 5 μM) or DMSO as indicated and Complete Growth Medium with cabozantinib (5 μM) or DMSO was added to the bottom wells. After 24 h, the invaded cells were stained and counted as described in Materials and methods. Data represent four independent experiments (**$P < 0.01$).

levels and elevated AXL, β-catenin and Snail protein levels (Figure 6b). Angiogenesis in pretreated tumors was elevated as demonstrated by increased human VEGF levels and CD31 levels (Figures 6b and c). The VEGF antibody we used is specific to human VEGF, which demonstrates that elevated levels of VEGF are from the human cell and not from the mice. The increased CD31 levels in pretreated tumors suggested that the overall number of CD31 expressing endothelial cells increased with sunitinib chronic pretreatment.

We generated our second xenograft model as described in Figure 6d. We injected 786-O cells subcutaneously into flanks of nude mice to generate tumors. When the tumors reached 200mm^3, we began administering sunitinib. In most cases, tumor growth moderated, followed by acceleration of growth while on sunitinib (Figure 6e). We examined the AXL and MET signaling cascade change in progressing tumors and discovered increased activity of these two signaling cascades (Figure 6f). Angiogenesis was also increased after 8 weeks of sunitinib treatment as suggested by increased human VEGF and CD31 levels (Figures 6f and g). At that point, we stopped administering sunitinib in half the animals and began administering cabozantinib to study the ability of cabozantinib to rescue sunitinib resistance. Treatment with cabozantinib rapidly reduced tumor size (Figure 6e). Cabozantinib suppressed both AXL/MET signaling cascades and

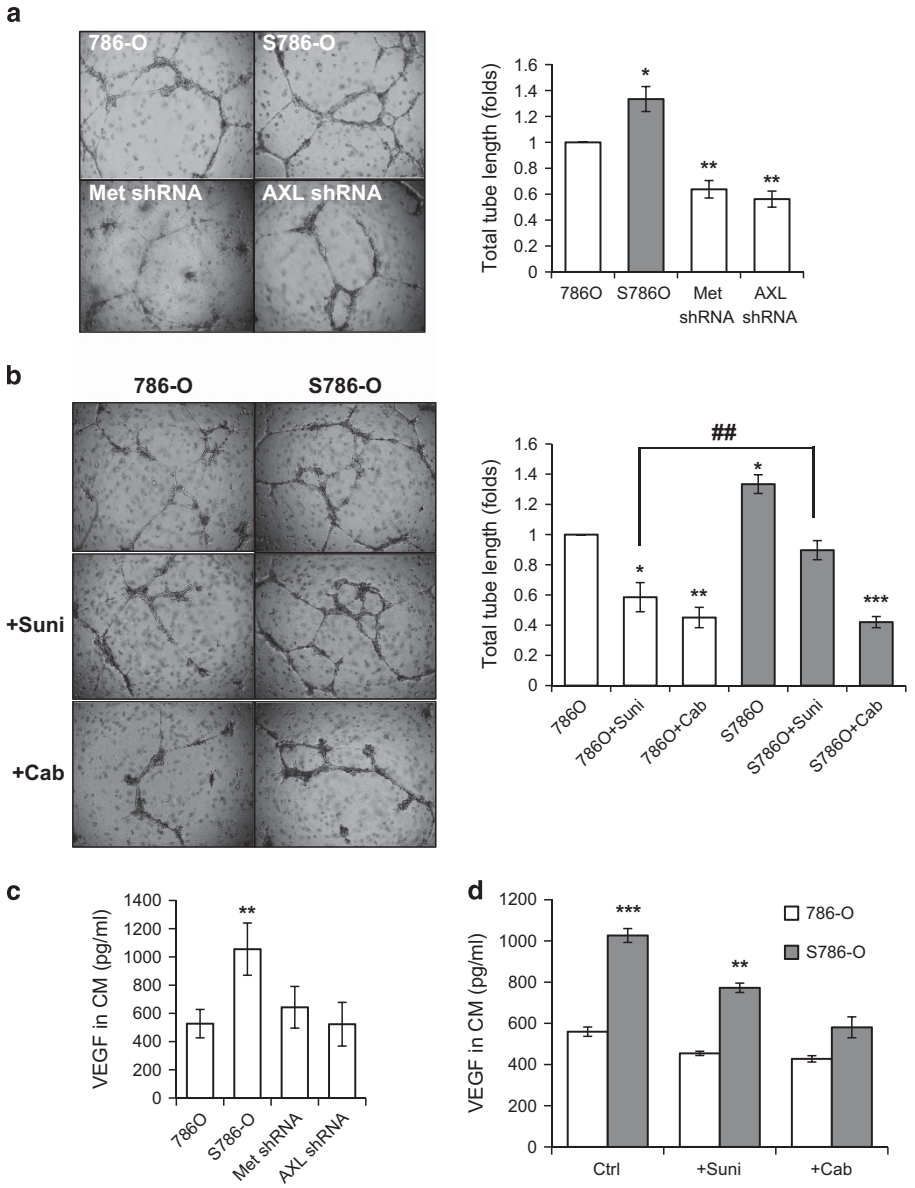

Figure 5. Chronic sunitinib treatment-induced AXL- and MET-dependent expression of VEGF and promoted HUVEC angiogenesis. (**a**) 786-O cells, 786-O cells that stably expressed *AXL* or *MET* shRNA constructs were chronically treated with sunitinib (1 μM) and then deprived of sunitinib, and 786-O parental cells were seeded (10 000 per well) in Matrigel (1:2 diluted) in 96-well plates, HUVEC cells were seeded on top of Matrigel (5000 per well). After 24 h, HUVEC cell tube formation was recorded with a bright field microscope. Data represent three independent experiments. The tube lengths were measured and quantified with the ImageJ software ($^{*}P < 0.05$, $^{**}P < 0.01$). (**b**) Chronic sunitinib-pretreated 786-O that were deprived of sunitinib (S786-O) or 786-O parental cells (10 000 per well) were seeded in Matrigel (1:2 diluted) in 96-well plates, HUVEC cells were seeded on top of Matrigel (5000 per well). The cell co-culture was treated with DMSO, sunitinib (+Suni, 1 μM) or cabozantinib (+Cab, 5 μM) for 24 h, and HUVEC tube formation was recorded with a bright field microscope. Data represent three independent experiments. The tube lengths were measured and quantified with the ImageJ software ($^{*}P < 0.05$, $^{**}P < 0.01$, $^{***}P < 0.001$, $^{\#\#}P < 0.01$). (**c**) 786-O cells, 786-O cells that were stably expressed with *AXL* or *MET* shRNA constructs were chronically treated with sunitinib (1 μM) and then deprived of sunitinib, and 786-O parental cells were cultured as described in Materials and methods. The conditioned media were collected and analyzed for VEGF levels. The results from four independent experiments were assessed for statistical significance ($^{**}P < 0.01$). (**d**) Chronic sunitinib-pretreated 786-O that were deprived of sunitinib (S786-O) or 786-O parental cells were cultured as described in Materials and methods. The conditioned media were collected and analyzed for VEGF concentration. The resulted from four independent experiments were assessed for statistical significance ($^{**}P < 0.01$). The data in this figure are representative for three shRNA constructs designed to target different sequences in *MET* and *AXL* ($^{**}P < 0.01$, $^{***}P < 0.001$).

tumor angiogenesis (Figures 6f and g). A schema summarizing our data is provided in Figure 6h.

DISCUSSION

RCC is one of the most lethal urological tumors because of the frequent development of metastatic disease to the lung, lymph nodes, bone, liver and brain, which reduces 5-year survival to approximately 10%. Antiangiogenic and mammalian target of rapamycin inhibitory agents are the major targeted therapies for RCC. These agents need to be given chronically or with minimal interruption, as discontinuation of antiangiogenic therapy results in the rapid onset of angiogenesis.[4] Unfortunately, antiangiogenic therapy almost universally leads to the development of resistance

and tumor progression, both in RCC and in other tumor types. In model systems of pancreatic neuroendocrine carcinoma and glioblastoma, tumors resistant to antiangiogenic therapy exhibit increased invasiveness as well as increased lymphatic and distant metastases.[42] Despite the use of these agents in thousands ;of patients to date, the mechanisms of resistance to antiangiogenic therapy are poorly understood.

High levels of AXL expression in primary RCC tumors are associated with shorter OS.[26] AXL signaling likely drives metastatic biology and is poorly targeted by existing agents. *In vitro* studies reported that sunitinib inhibits AXL with an IC50 of 259 nM.[43] Additionally, elevated AXL protein expression and kinase activation were observed in non-small cell lung cancers after treatment with antiangiogenic therapy.[44] Our current study demonstrates

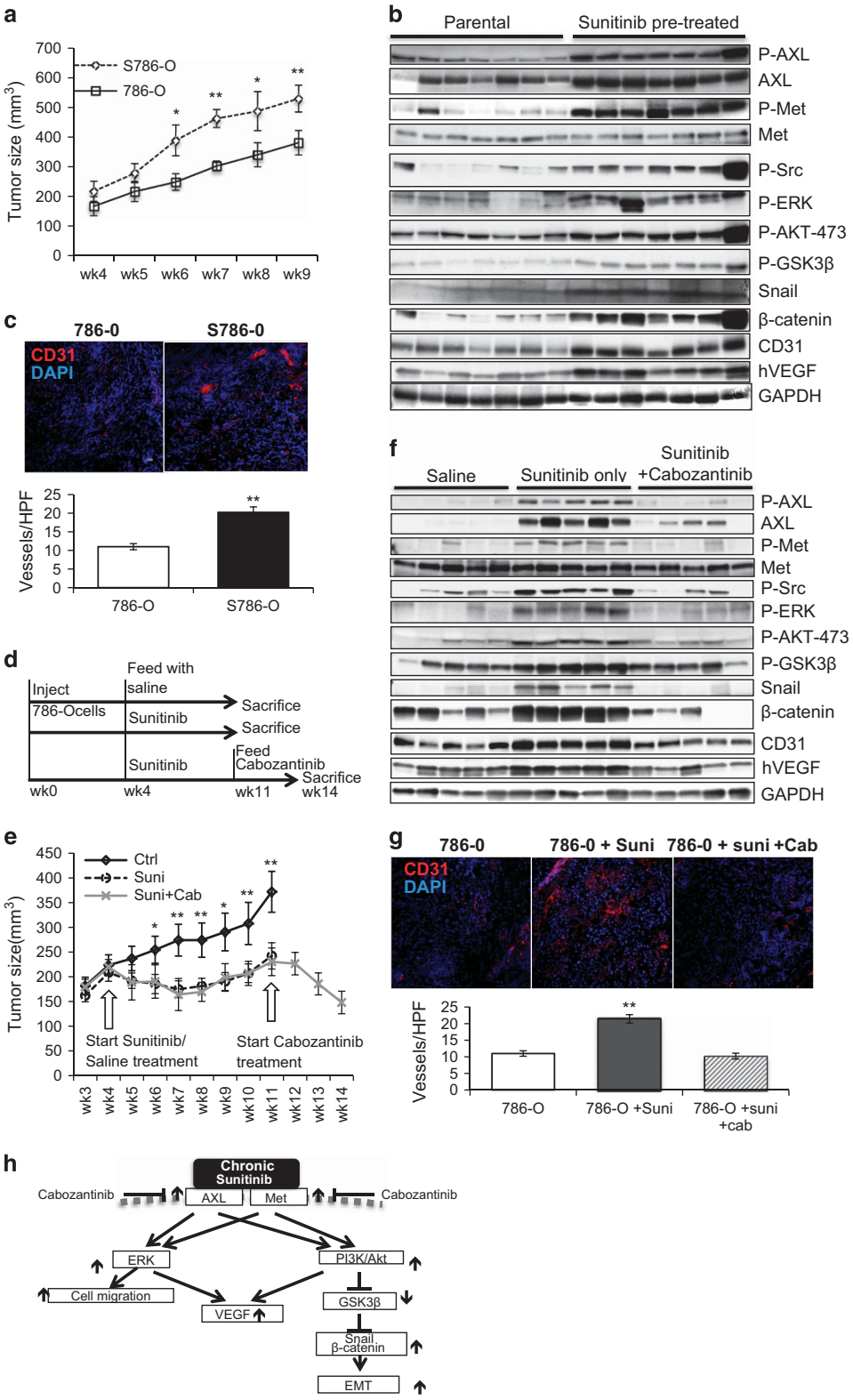

that, after chronic pretreatment with sunitinib, the AXL protein level is elevated in patient samples (Figure 1) and activity of AXL is increased in RCC cell lines (Figure 2) and xenograft tumors (Figures 6b and f). High MET expression is also associated with adverse pathological features (higher Fuhrman grade and more advanced disease stage) and poor prognosis.[13] In our present study, we observed that acute sunitinib treatment suppressed MET activity, but with chronic treatment MET activity recovered. Following removal of sunitinib after chronic treatment, MET and AXL activity remained increased (Figure 2a). The activation of these two kinases resulted in the stimulation of their downstream signaling cascades and promoted EMT signaling. By shRNA knockdown of either AXL or MET, we observed that increased cell migration and invasion induced by chronic sunitinib treatment were AXL and MET dependent. In addition to the gain of EMT properties, we also observed increased angiogenesis, which was stimulated in part by increased VEGF secretion from the tumor cell as suggested by both cell culture experiments (Figure 5) and xenograft tumor experiments (Figure 6). But whether elevated VEGF level alone is sufficient to overcome the inhibitory effect of sunitinib on VEGF receptor on epithelial cells remain to be studied.

Cabozantinib is an inhibitor of tyrosine kinases, including VEGF receptors MET and AXL, which is being investigated in a range of human cancers, including RCC. We examined the ability of cabozantinib to suppress chronic sunitinib treatment-induced EMT in our study. Our results suggest that cabozantinib can inhibit the activation of AXL and MET in RCC cells with or without sunitinib pretreatment (Figure 4). This effect is also observed in the treatment of xenograft tumors that were pretreated with sunitinib (Figure 6f). Cabozantinib can suppress chronic sunitinib pretreatment-induced AKT, ERK, EMT signaling activation, cell migration and invasion (Figures 4 and 6). In addition, cabozantinib is able to suppress chronic sunitinib treatment-induced angiogenesis by suppressing VEGF secretion from RCC cells or production in xenograft tumors.

Lytic bone metastases are a particularly troublesome manifestation of metastatic RCC. Clinical observations and both published[45] and unpublished data suggest that RCC patients treated with antiangiogenic therapy tend not to show a high rate of response in bone. The emerging data from prostate cancer patients treated with cabozantinib[46] raises the intriguing possibility that resistance to antiangiogenic therapy in RCC may be due to upregulation of MET in the bone microenvironment. Therefore, downregulation of MET by pharmacological means may be a rational therapeutic strategy for investigation in this patient population. Our findings suggest that further investigation of cabozantinib in patients with lytic bone metastases may also be warranted.

In summary, our study revealed that chronic sunitinib treatment of RCC cell lines and xenograft tumors induced AXL- and MET-mediated cellular EMT and VEGF secretion and activated ERK and PI3K/AKT signaling. These findings provide a potential explanation for the underlying mechanism of resistance to sunitinib treatment and suggest that investigation of agents targeting AXL and MET in antiangiogenic therapy-resistant RCC patients could represent a new therapeutic approach.

MATERIALS AND METHODS

Human tissue microarrays

A Beecher tissue microarrayer (Estigen Inc., Tartu, Estonia) was used to generate triplicate 0.6-mm cores from formalin-fixed paraffin-embedded primary clear cell RCC tumor samples from patients with metastatic disease treated on three separate clinical trials: NCT00113217, NCT00715442, and NCT00126594.[6,47] These cores were used to generate a tissue microarray. A total of 40 cases of primary, untreated RCC and 39 cases of primary, sunitinib pretreated and tumors were included in the arrays and in the analysis. Informed consent was obtained for all patients. None of the patients were pretreated with other agents. Using a Vectra Multispectral imager (Perkin Elmer, Waltham, MA, USA) and published quantitation methods, the levels of AXL and MET in those treated and untreated samples were blinded, quantified and then matched with patient data to be analyzed. The inForm algorithm was trained by a pathologist (Kanishka Sircar) to exclude stroma from immunohistochemical analysis and to provide a quantifiable readout of AXL and MET expression. The differences of MET and AXL staining among tissues were evaluated by Student's *t*-test. Data represent mean ± s.e.m. $P < 0.05$ was considered significant.

Antibodies and reagents

Antibodies against AXL (no. 8661), phospho-AXL (Tyr702) (no. 5724), phospho-MET (Tyr1234/1235) (no. 3077), AKT (no. 4685), phospho-AKT (ser473) (no. 4058), ERK (no. 4696), phospho-ERK (Thr202/Tyr204) (4376), GSK3β (9832), phospho-GSK3β (Ser9) (no. 5558), β-catenin (no. 8480), Snail (no. 3879) and phospho-Src-Y416 (no. 6943) were purchased from Cell Signaling Technology (Danvers, MA, USA). Antibody against Met (sc-161-R) was purchased from Santa Cruz Biotechnology (Santa Cruz, CA, USA). Antibody against AXL (no. AF154) purchased from R&D Systems (Minneapolis, MN, USA) was used for immunohistochemistry. Antibodies against VEGF (ab150766) and CD31 (ab28364) were purchased from Abcam (Cambridge, MA, USA). Recombinant GAS6 (no. 885-GS-050) was purchased from R&D Systems. Recombinant HGF (no. GF116) was purchased from Millipore (Billerica, MA, USA). Mitomycin C (no. 475820) was purchased from Calbiochem (Billerica, MA, USA). Sunitinib (no. s1042) was purchased from Selleckchem (Houston, TX, USA). Cabozantinib was provided by Exelixis (South San Francisco, CA, USA).

Cell lines and culture conditions, plasmids and lentivirus generation

All of the cells used in this study were cultured in 37 °C incubator with 5% CO_2. 786-O cells and the cells derived from 786-O cells were cultured in Dulbecco's modified Eagle's medium (DMEM) supplied with 10% fetal bovine serum (FBS). A498 and RCC4 cells were cultured in DMEM supplied with 10% FBS. Cells were routinely monitored for mycoplasma contamination. AXL (clone ID V2LHS_238359, V3LHS_329653 and V3LHS_329651) and Met (clone ID V2LHS_76544, V2LHS_76542, V3LHS_646098) shRNA plasmids were obtained from Openbiosystems (Huntsville, AL, USA). The AXL and Met shRNA lentivirus were generated with the MISSION Lentiviral Packaging Mix (no. SHP001) from Sigma-Aldrich (St Louis, MO, USA) according to the manufacturer's instruction. HUVEC cells were cultured in

Figure 6. Chronic sunitinib treatment-induced AXL and MET signaling and angiogenesis in xenograft mouse models. (**a**) 1×10^7 786-O cells (786-O) or chronic sunitinib-pretreated 786-O (S786-O) were injected into the flank of each NCr-nu/nu mouse (10 mice per group). The xenograft tumor sizes were measured after 4 weeks' stabilization. The size difference between two groups at the same time point was analyzed using Student's *t*-test. (*$P < 0.05$, **$P < 0.01$). (**b**) The mice were killed after 9 weeks, the tumor tissue was obtained and equal amounts of protein lysate were analyzed by western blotting with specific antibodies as indicated. (**c**) Representative immunohistochemistry staining of CD31 (red) and cell nucleus (DAPI (4,6-diamidino-2-phenylindole), blue) in xenograft tumor sections from the experiment performed in panel (**b**). (**d**) Diagram describes the experimental design of *in vivo* sunitinib-resistant (20 mg/kg, daily) tumor generation followed with cabozantinib (40 mg/kg, daily) treatment (10 mice per group). (**e**) The measurement of tumor size during the experiment of panel (**d**). The size difference between the sunitinib- and saline-treated groups at the same time point was analyzed using Student's *t*-test. (*$P < 0.05$, **$P < 0.01$). (**f**) The mice were killed after saline/sunitinib or cabozantinib treatment, the tumor tissue were obtained and equal amount of protein lysate were analyzed by western blotting with specific antibodies as indicated. (**g**) Representative immunohistochemistry staining of CD31 (red) and cell nucleus (DAPI, blue) in xenograft tumor sections from the experiment performed in panel (**f**). (**h**) Proposed model for chronic sunitinib treatment-induced drug resistance.

medium 200 (no. M-200-500, Life Technologies, Grand Island, NY, USA) supplied with 2% LSGS (#S-003-10, Life Technologies).

Scratch wound-healing assay

Cells were seeded to reach ~90% confluence 24 h before experiment. The cell monolayers were scratched with a 1-ml tip and switched to a medium containing Mitomycin C (0.02 mg/ml) (Sigma-Aldrich) and reagents specified in each experiment. Twenty-four hours postscratch, cells were fixed with methanol and stained with crystal blue. The gap pictures were captured with an Olympus BX43 microscope (Tokyo, Japan) that was equipped with an Olympus DP21 camera (Tokyo, Japan). The gap distance was measured with the ImageJ software (NIH, Bethesda, MD, USA). Cell migration distances between cell groups were compared using Student's *t*-test. Data represent mean ± s.e.m. $P < 0.05$ was considered significant.

Cell survival curve

Cells were seeded 24 h in advance; the designated therapeutic agents were then applied. Twenty-four hours after treatment, the total cell numbers (*T*) were counted using an In-Cell 6000 system (GE Healthcare, Pittsburgh, PA, USA) with Hoechst 33258 (861405 Sigma-Aldrich) staining representing the total cell number. The dead cell numbers (*D*) were counted by staining with DRAQ-7 (ab109202, Abcam). Living cell number (*L*) was calculated by subtracting dead cell number from total cell number ($L = T - D$). The live cell ratio were calculated by using $L_{treated}/L_{control}$ (%) and plotted with dose (μM). A ×4 objective was used for image capture. The images were analyzed with the IN Cell Analyzer software (GE Healthcare). The statistical difference of cell number change after different treatments was determined using Student's *t*-test. Data represent mean ± s.e.m. $P < 0.05$ was considered significant.

Cell invasion

Matrigel (no. 354248, Corning, Bedford, MA, USA) was diluted in a 1:5 ratio with DMEM medium and coated on the transwell (no. CLS3422, Sigma-Aldrich). Five thousand cells per well were seeded on the Matrigel in transwells in DMEM medium without FBS. DMEM supplied with 10% FBS was used as a chemoattractant. After 24 h, the invading cells were stained with Crystal Blue. Cell images were captured on an Olympus BX43 microscope that was equipped with an Olympus DP21 camera. The cell images were analyzed for cell numbers with the ImageJ software (NIH). Statistical difference of cell number change with different treatments was determined by using Student's *t*-test. Data represent mean ± s.e.m. $P < 0.05$ was considered significant.

Measurement of VEGF

Human VEGF ELISA Kit was purchased from Thermo Scientific (Cat. no. EH2VEGF). In all, 5×10^4 cells were plated in each well of a 12-well plate in a medium volume of 1ml/well. After 24 h, the cells were treated with different chemicals as indicated in the figure legends for a further 24 h. The conditioned media were collected and analyzed it for VEGF concentration according to the manufacturer's instruction. Statistical significance of HUVEC tube length change after different treatments was analyzed by using Student's *t*-test. Data represent mean ± s.e.m. $P < 0.05$ was considered significant.

Xenograft tumor models

The University of Texas MD Anderson Cancer Center Institutional Animal Care and Use Committee approved all experiments. To generate *in vivo* sunitinib-resistant tumors, we injected 1×10^7 786-O RCC cells into the flanks of 4-week-old NCr-nu/nu mice. Total mice number was 30. After tumors became palpable (that is, tumor volume reached 200 mm^3), randomly picked (by using a random number table) 20 tumor-bearing mice were treated with sunitinib (20 mg/kg) by oral gavage daily until the tumors resumed growth. Ten randomly picked mice were treated with saline by oral gavage as control. Then half (10) of the mice were switched to cabozantinib treatment for 40 mg/kg by gavage daily. The mice were then killed when planned treatment course was complete. Tumor tissue was collected for further analysis following standard procedures. For the side-to-side comparison of the sustained effect of *ex-vivo* chronic sunitinib treatment, sunitinib pretreated 786-O cells or parental 786-O cells were injected into the left or right flank of 10 NCr-nu/nu mice as described above. The tumor sizes were monitored for 9 weeks. The mice were then killed, and tumor tissue was collected for analysis.

Animal health was assessed daily to minimize pain and distress. Veterinary staff monitored mice for tumor burden, behavioral changes and appetite changes. The tumor size change between different groups was evaluated using Student's *t*-test. Data represent mean ± s.e.m. $P < 0.05$ was considered significant.

Immunohistochemistry of xenograft tumor tissue

Acetone-fixed frozen xenograft tissue sections were used for CD31 immuno-detection. Images were captured with Vectra Multispectral imager. The CD31-positive area were counted as described previously.[48] Ten images per tumor were analyzed.

CONFLICT OF INTEREST

Dr Jonasch has received research funding from Pfizer, Novartis, GSK, Onyx and Exelixis. Dr Jonasch is a consultant for Pfizer, GSK, Novartis and Genentech. The other authors declare no conflict of interest.

ACKNOWLEDGEMENTS

This work was supported by Exelixis, Renee Kaye Cure Fur Cancer Foundation, the Monteleone Family Foundation and the UT MD Anderson Cancer Center P30 Cancer Center Support Grant.

REFERENCES

1 Thoenes W, Storkel S, Rumpelt HJ. Histopathology and classification of renal cell tumors (adenomas, oncocytomas and carcinomas). The basic cytological and histopathological elements and their use for diagnostics. *Pathol Res Pract* 1986; **181**: 125–143.
2 Kanesvaran R, Tan MH. Targeted therapy for renal cell carcinoma: The next lap. *J Carcinog* 2014; **13**: 3.
3 Domblides C, Gross-Goupil M, Quivy A, Ravaud A. Emerging antiangiogenics for renal cancer. *Expert Opin Emerg Drugs* 2013; **18**: 495–511.
4 Griffioen AW, Mans LA, de Graaf AM, Nowak-Sliwinska P, de Hoog CL, de Jong TA *et al.* Rapid angiogenesis onset after discontinuation of sunitinib treatment of renal cell carcinoma patients. *Clin Cancer Res* 2012; **18**: 3961–3971.
5 Huang D, Ding Y, Zhou M, Rini BI, Petillo D, Qian CN *et al.* Interleukin-8 mediates resistance to antiangiogenic agent sunitinib in renal cell carcinoma. *Cancer Res* 2010; **70**: 1063–1071.
6 Jonasch E, Corn P, Pagliaro LC, Warneke CL, Johnson MM, Tamboli P *et al.* Upfront, randomized, phase 2 trial of sorafenib versus sorafenib and low-dose interferon alfa in patients with advanced renal cell carcinoma: clinical and biomarker analysis. *Cancer* 2010; **116**: 57–65.
7 Tsavachidou-Fenner D, Tannir N, Tamboli P, Liu W, Petillo D, Teh B *et al.* Gene and protein expression markers of response to combined antiangiogenic and epidermal growth factor targeted therapy in renal cell carcinoma. *Ann Oncol* 2010; **21**: 1599–1606.
8 Kim J, Jonasch E, Alexander A, Short JD, Cai S, Wen S *et al.* Cytoplasmic sequestration of p27 via AKT phosphorylation in renal cell carcinoma. *Clin Cancer Res* 2009; **15**: 81–90.
9 Rankin EB, Fuh KC, Castellini L, Viswanathan K, Finger EC, Diep AN *et al.* Direct regulation of GAS6/AXL signaling by HIF promotes renal metastasis through SRC and MET. *Proc Natl Acad Sci USA* 2014; **111**: 13373–13378.
10 Peters S, Adjei AA. MET: a promising anticancer therapeutic target. *Nat Rev Clin Oncol* 2012; **9**: 314–326.
11 Birchmeier C, Birchmeier W, Gherardi E, Vande Woude GF. Met metastasis, motility and more. *Nat Rev Mol Cell Biol* 2003; **4**: 915–925.
12 Gherardi E, Birchmeier W, Birchmeier C, Vande Woude G. Targeting MET in cancer: rationale and progress. *Nat Rev Cancer* 2012; **12**: 89–103.
13 Gibney GT, Aziz SA, Camp RL, Conrad P, Schwartz BE, Chen CR *et al.* c-Met is a prognostic marker and potential therapeutic target in clear cell renal cell carcinoma. *Ann Oncol* 2013; **24**: 343–349.
14 Miyata Y, Kanetake H, Kanda S. Presence of phosphorylated hepatocyte growth factor receptor/c-Met is associated with tumor progression and survival in patients with conventional renal cell carcinoma. *Clin Cancer Res* 2006; **12**: 4876–4881.
15 Betsunoh H, Mukai S, Akiyama Y, Fukushima T, Minamiguchi N, Hasui Y *et al.* Clinical relevance of hepsin and hepatocyte growth factor activator inhibitor type 2 expression in renal cell carcinoma. *Cancer Sci* 2007; **98**: 491–498.
16 Sennino B, Ishiguro-Oonuma T, Wei Y, Naylor RM, Williamson CW, Bhagwandin V *et al.* Suppression of tumor invasion and metastasis by concurrent

inhibition of c-Met and VEGF signaling in pancreatic neuroendocrine tumors. *Cancer Discov* 2012; **2**: 270–287.
17 Rankin EB, Fuh KC, Taylor TE, Krieg AJ, Musser M, Yuan J *et al.* AXL is an essential factor and therapeutic target for metastatic ovarian cancer. *Cancer Res* 2010; **70**: 7570–7579.
18 Ye X, Li Y, Stawicki S, Couto S, Eastham-Anderson J, Kallop D *et al.* An anti-Axl monoclonal antibody attenuates xenograft tumor growth and enhances the effect of multiple anticancer therapies. *Oncogene* 2010; **29**: 5254–5264.
19 Holland SJ, Powell MJ, Franci C, Chan EW, Friera AM, Atchison RE *et al.* Multiple roles for the receptor tyrosine kinase axl in tumor formation. *Cancer Res* 2005; **65**: 9294–9303.
20 Linger RM, Keating AK, Earp HS, Graham DK. TAM receptor tyrosine kinases: biologic functions, signaling, and potential therapeutic targeting in human cancer. *Adv Cancer Res* 2008; **100**: 35–83.
21 Linger RM, Keating AK, Earp HS, Graham DK. Taking aim at Mer and Axl receptor tyrosine kinases as novel therapeutic targets in solid tumors. *Expert Opin Ther Targets* 2010; **14**: 1073–1090.
22 Gujral TS, Karp RL, Finski A, Chan M, Schwartz PE, Macbeath G *et al.* Profiling phospho-signaling networks in breast cancer using reverse-phase protein arrays. *Oncogene* 2012; **32**: 3470–3476.
23 Zhang Z, Lee JC, Lin L, Olivas V, Au V, Laframboise T *et al.* Activation of the AXL kinase causes resistance to EGFR-targeted therapy in lung cancer. *Nat Genet* 2012; **44**: 852–860.
24 Ruan GX, Kazlauskas A. Axl is essential for VEGF-A-dependent activation of PI3K/Akt. *EMBO J* 2012; **31**: 1692–1703.
25 Chung BI, Malkowicz SB, Nguyen TB, Libertino JA, McGarvey TW. Expression of the proto-oncogene Axl in renal cell carcinoma. *DNA Cell Biol* 2003; **22**: 533–540.
26 Gustafsson A, Martuszewska D, Johansson M, Ekman C, Hafizi S, Ljungberg B *et al.* Differential expression of Axl and Gas6 in renal cell carcinoma reflecting tumor advancement and survival. *Clin Cancer Res* 2009; **15**: 4742–4749.
27 Pao-Chun L, Chan PM, Chan W, Manser E. Cytoplasmic ACK1 interaction with multiple receptor tyrosine kinases is mediated by Grb2: an analysis of ACK1 effects on Axl signaling. *J Biol Chem* 2009; **284**: 34954–34963.
28 Leconet W, Larbouret C, Chardes T, Thomas G, Neiveyans M, Busson M *et al.* Preclinical validation of AXL receptor as a target for antibody-based pancreatic cancer immunotherapy. *Oncogene* 2014; **33**: 5405–5414.
29 Gustafsson A, Bostrom AK, Ljungberg B, Axelson H, Dahlback B. Gas6 and the receptor tyrosine kinase Axl in clear cell renal cell carcinoma. *PLoS One* 2009; **4**: e7575.
30 Horie S, Aruga S, Kawamata H, Okui N, Kakizoe T, Kitamura T. Biological role of HGF/MET pathway in renal cell carcinoma. *J Urol* 1999; **161**: 990–997.
31 Ellison AR, Lofing J, Bitter GA. Potentiation of human estrogen receptor alpha-mediated gene expression by steroid receptor coactivator-1 (SRC-1) in *Saccharomyces cerevisiae*. *J Steroid Biochem Mol Biol* 2003; **86**: 15–26.
32 Rahimi N, Hung W, Tremblay E, Saulnier R, Elliott B. c-Src kinase activity is required for hepatocyte growth factor-induced motility and anchorage-independent growth of mammary carcinoma cells. *J Biol Chem* 1998; **273**: 33714–33721.
33 Singhal E, Sen P. Hepatocyte growth factor-induced c-Src-phosphatidylinositol 3-kinase-AKT-mammalian target of rapamycin pathway inhibits dendritic cell activation by blocking IkappaB kinase activity. *Int J Biochem Cell Biol* 2011; **43**: 1134–1146.
34 Ho MY, Tang SJ, Chuang MJ, Cha TL, Li JY, Sun GH *et al.* TNF-alpha induces epithelial-mesenchymal transition of renal cell carcinoma cells via a GSK3beta-dependent mechanism. *Mol Cancer Res* 2012; **10**: 1109–1119.
35 Garofalo M, Romano G, Di Leva G, Nuovo G, Jeon YJ, Ngankeu A *et al.* EGFR and MET receptor tyrosine kinase-altered microRNA expression induces tumorigenesis and gefitinib resistance in lung cancers. *Nat Med* 2012; **18**: 74–82.
36 Friedl P, Alexander S. Cancer invasion and the microenvironment: plasticity and reciprocity. *Cell* 2011; **147**: 992–1009.
37 Harshman LC, Choueiri TK. Targeting the hepatocyte growth factor/c-Met signaling pathway in renal cell carcinoma. *Cancer J* 2013; **19**: 316–323.
38 Chinchar E, Makey KL, Gibson J, Chen F, Cole SA, Megason GC *et al.* Sunitinib significantly suppresses the proliferation, migration, apoptosis resistance, tumor angiogenesis and growth of triple-negative breast cancers but increases breast cancer stem cells. *Vasc Cell* 2014; **6**: 12.
39 Choueiri TK, Pal SK, McDermott DF, Morrissey S, Ferguson KC, Holland J *et al.* A phase I study of cabozantinib (XL184) in patients with renal cell cancer. *Ann Oncol* 2014; **25**: 1603–1608.
40 Bentzien F, Zuzow M, Heald N, Gibson A, Shi Y, Goon L *et al.* In vitro and in vivo activity of cabozantinib (XL184), an inhibitor of RET, MET, and VEGFR2, in a model of medullary thyroid cancer. *Thyroid* 2013; **23**: 1569–1577.
41 Zhang Y, Guessous F, Kofman A, Schiff D, Abounader R. XL-184, a MET, VEGFR-2 and RET kinase inhibitor for the treatment of thyroid cancer, glioblastoma multiforme and NSCLC. *IDrugs* 2010; **13**: 112–121.
42 Paez-Ribes M, Allen E, Hudock J, Takeda T, Okuyama H, Vinals F *et al.* Antiangiogenic therapy elicits malignant progression of tumors to increased local invasion and distant metastasis. *Cancer Cell* 2009; **15**: 220–231.
43 Kumar R, Crouthamel MC, Rominger DH, Gontarek RR, Tummino PJ, Levin RA *et al.* Myelosuppression and kinase selectivity of multikinase angiogenesis inhibitors. *Br J Cancer* 2009; **101**: 1717–1723.
44 Zhang Z, Lee JC, Lin L, Olivas V, Au V, LaFramboise T *et al.* Activation of the AXL kinase causes resistance to EGFR-targeted therapy in lung cancer. *Nat Genet* 2012; **44**: 852–860.
45 Plimack ER, Tannir N, Lin E, Bekele BN, Jonasch E. Patterns of disease progression in metastatic renal cell carcinoma patients treated with antivascular agents and interferon: impact of therapy on recurrence patterns and outcome measures. *Cancer* 2009; **115**: 1859–1866.
46 Smith DC, Smith MR, Sweeney C, Elfiky AA, Logothetis C, Corn PG *et al.* Cabozantinib in patients with advanced prostate cancer: results of a phase II randomized discontinuation trial. *J Clin Oncol* 2013; **31**: 412–419.
47 Jonasch E, Wood CG, Matin SF, Tu SM, Pagliaro LC, Corn PG *et al.* Phase II presurgical feasibility study of bevacizumab in untreated patients with metastatic renal cell carcinoma. *J Clin Oncol* 2009; **27**: 4076–4081.
48 Weidner N. Intratumor microvessel density as a prognostic factor in cancer. *Am J Pathol* 1995; **147**: 9–19.

Supplementary Information accompanies this paper on the Oncogene website (http://www.nature.com/onc)